

## Orbital symmetry reconstruction and strong mass renormalization in the two-dimensional electron gas at the surface of $\text{KTaO}_3$

A. F. Santander-Syro,<sup>1,2,\*</sup> C. Bareille,<sup>1</sup> F. Fortuna,<sup>1</sup> O. Copie,<sup>3,†</sup> M. Gabay,<sup>4</sup> F. Bertran,<sup>5</sup> A. Taleb-Ibrahimi,<sup>5</sup> P. Le Fèvre,<sup>5</sup> G. Herranz,<sup>6</sup> N. Reyren,<sup>7,8</sup> M. Bibes,<sup>7,8</sup> A. Barthélémy,<sup>7,8</sup> P. Lecoeur,<sup>9</sup> J. Guevara,<sup>10</sup> and M. J. Rozenberg<sup>4</sup>

<sup>1</sup>CSNSM, Université Paris-Sud and CNRS/IN2P3, Bâtiments 104 et 108, 91405 Orsay cedex, France

<sup>2</sup>Laboratoire Physique et Etude des Matériaux, UMR-8213 ESPCI/UPMC/CNRS, 10 rue Vauquelin, 75231 Paris cedex 5, France

<sup>3</sup>Universität Würzburg, Experimentelle Physik VII, 97074 Würzburg, Germany

<sup>4</sup>Laboratoire de Physique des Solides, Université Paris-Sud, Bâtiment 510, 91405 Orsay, France

<sup>5</sup>Synchrotron SOLEIL, L'Orme des Merisiers, Saint-Aubin Boîte Postale 48, 91192 Gif-sur-Yvette, France

<sup>6</sup>Institut de Ciència de Materials de Barcelona, CSIC, Campus de la UAB, 08193 Bellaterra, Catalunya, Spain

<sup>7</sup>Unité Mixte de Physique CNRS/Thales, Campus de l'École Polytechnique, 1 Avenue A. Fresnel, 91767 Palaiseau, France

<sup>8</sup>Université Paris-Sud, 91405 Orsay, France

<sup>9</sup>Institut d'Electronique Fondamentale, Université Paris-Sud, Bâtiment 220, 91405 Orsay, France

<sup>10</sup>Escuela de Ciencia y Tecnología, Universidad de San Martín, and CONICET, Argentina

(Received 13 July 2012; revised manuscript received 31 August 2012; published 19 September 2012)

We study, using angle-resolved photoemission spectroscopy, the two-dimensional electron gas (2DEG) at the surface of  $\text{KTaO}_3$  (KTO), a wide-gap insulator with strong spin-orbit coupling (SOC). We find that this 2DEG is a genuinely different physical state with respect to the bulk: the orbital symmetries of its subbands are entirely reconstructed and their masses are renormalized. This occurs because the values of the SOC, the Fermi energy, and the subband splittings become comparable in the 2DEG. Additionally, we identify an  $F$ -center-like heavy band resulting from the polar nature of the KTO surface.

DOI: [10.1103/PhysRevB.86.121107](https://doi.org/10.1103/PhysRevB.86.121107)

PACS number(s): 73.20.At, 73.22.-f, 77.84.Ek

The discovery of a high-mobility two-dimensional electron gas (2DEG) at the interface of two nonmagnetic wide-band-gap oxide insulators,  $\text{SrTiO}_3$  (STO) and  $\text{LaAlO}_3$  (LAO),<sup>1</sup> triggered a burst of activity that led to more surprising findings in STO-based interfaces, such as superconductivity,<sup>2,3</sup> fingerprints of ferromagnetism,<sup>4,5</sup> and large magnetoresistance.<sup>6–8</sup> However, the physical origin of these metallic states remains unanswered.<sup>9–12</sup> This was underscored by the finding that a 2DEG is formed at the surface of vacuum-cleaved crystals of STO,<sup>13,14</sup> opening another avenue for the understanding and fabrication of 2DEGs in transition-metal oxides. It was argued that this novel state arises from surface oxygen vacancies, demonstrating that different forms of electron confinement at the surface of STO lead to essentially the same 2DEG.<sup>13</sup>

Indeed, the prospect of creating 2DEGs at the surface of other multifunctional oxides which may inherit the properties of their parent compounds is exciting.<sup>13</sup> Here we focus on  $\text{KTaO}_3$  (KTO), a wide-gap  $5d^0$  insulator presenting a strong ( $\sim 0.47$  eV) spin-orbit coupling (SOC), more than one order of magnitude larger than in STO.<sup>15</sup> As transport experiments have shown, gating samples of this material produced confined metallic states displaying large magnetoresistance<sup>16</sup> and superconductivity below 50 mK.<sup>17</sup> Additionally, very recent angle-resolved photoemission spectroscopy (ARPES) experiments reported the realization of a 2DEG directly at the vacuum-cleaved surface of KTO.<sup>18</sup>

In the present work, we go further and demonstrate that the 2DEG at the surface of KTO is, in contrast to the case of STO-based 2DEGs, a genuinely different physical system with respect to the bulk: the orbital symmetries of the surface subbands are reconstructed, and their masses are significantly renormalized. We show that this occurs because the Fermi energy and subband splittings in the confined electron gas

are comparable in magnitude to the SOC interaction, an unconventional situation not present in the STO-based 2DEGs. These findings demonstrate how, in multifunctional oxides, the strong couplings between the active electronic degrees of freedom, combined with the electron confinement, can lead to electronic states not present in the bulk. In addition, we identify an  $F$ -center-like heavy band stemming from the polar nature of the KTO surface, implying that different surface terminations can serve to control the physical properties of the 2DEG.

The high-quality *undoped* transparent single crystals of  $\text{KTaO}_3$  were studied through ARPES at the Synchrotron Radiation Center (University of Wisconsin, Madison) and at SOLEIL (France). The sample preparation and measurement are detailed in the Supplemental Material.<sup>19</sup>

Figure 1 serves as a convenient guide to our data analysis. To understand the electron states at the surface of  $\text{KTaO}_3$ , one must consider the combined effects of the strong SOC and of the 2D confinement along the (001) direction (defined as  $z$ ). For simplicity, we shall first consider only the lowest-energy subbands of different orbital characters. In the bulk [Fig. 1(a)], the SOC splits the degenerate  $t_{2g}$  bands at  $\Gamma$  by the spin-orbit gap  $\Delta_{SO}$  into a low-lying quartet ( $\psi_1, \psi_2, \psi_3, \psi_4$ ) derived from the  $J = 3/2$  states, composed of a heavy ( $E_{hb}$ ) and a light ( $E_{lb}$ ) band, plus a higher-energy doublet ( $\psi_5, \psi_6$ ) derived from the  $J = 1/2$  states forming a band ( $E_{so}$ ) with a light mass.<sup>19–23</sup> Due to SOC, the resulting bands have mixed orbital characters (Table I, “Bulk” entries), which need to be taken into account to understand the unusual effects of confinement on this material. The tight-binding calculations of Fig. 1(a) and Table I (see also the  $\mathbf{k} \cdot \mathbf{p}$  calculations in Ref. 19) show that, while the heavy bulk band along  $y$  has a strong  $d_{xz}$  character, thus being light along the  $z$  axis,<sup>13</sup> its partner light band in the doublet is essentially an equal admixture of  $d_{xy}$  and  $d_{yz}$

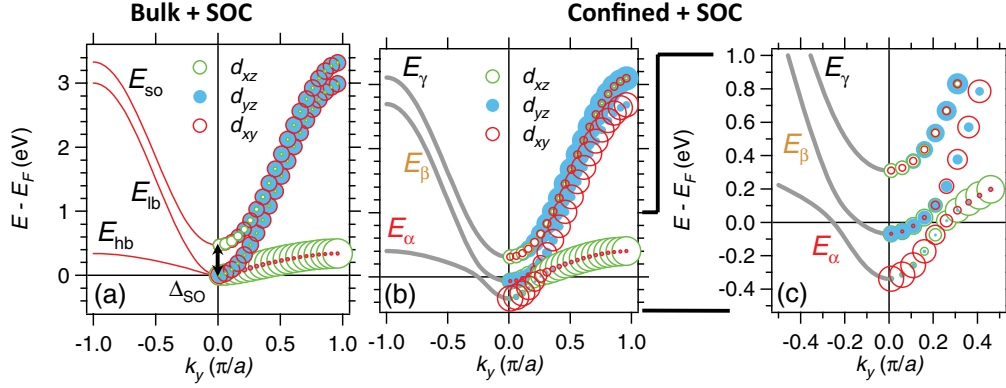


FIG. 1. (Color online) (a) Tight-binding model calculations for bulk KTaO<sub>3</sub> (red lines, left). The nearest-neighbor hopping parameters are  $t = 1.5$  eV and  $t' = 0.15$  eV for the light and heavy bands, respectively. The Fermi level is arbitrarily set to the conduction band minimum. For each band, the weights of the  $d_{xy}$ ,  $d_{yz}$ , and  $d_{xz}$  orbital characters are proportional to the sizes of the red, blue, and green circles, respectively (right). (b), (c) Effect of confinement on subbands  $n = 1$  (gray lines) and on their orbital characters (circles). The Fermi level is set to fit the experimental band filling (see main text).

characters, which are respectively heavy and light along  $z$ . In the 2DEG [Figs. 1(b) and 1(c)], each of the  $t_{2g}$  orbital components of every band acquires a different “zero-point energy,” inversely proportional to its respective  $z$ -axis mass. It is crucial to realize that these  $z$ -axis masses correspond to those of the bulk bands *in the absence of SOC*, which for KTO can be estimated from local density approximation (LDA) calculations to be about  $5m_e$  and  $0.3m_e$  for the  $d_{xy}$  and  $d_{xz/yz}$  bands, respectively.<sup>19</sup> In other words, confinement “lifts up” the *pure*  $t_{2g}$  light orbital components with respect to the heavy ones. This not only modifies the relative ordering of the bands, as in the simpler case of STO,<sup>13</sup> but now completely *changes* the orbital symmetries of the bands in the 2DEG with respect to the bulk, as summarized in Table I (“2DEG” entries). This results in a strongly  $k$ -dependent orbital mixing and a dramatic change in the in-plane effective masses, as shown in Figs. 1(b) and 1(c) and Table I. In particular, near the  $\Gamma$  point, the band with a heavy mass in the bulk becomes much lighter as it acquires a strong  $d_{xy}$  character. We label this lowest-lying subband  $E_\alpha$ . On the other hand, the next subband of different symmetry, labeled  $E_\beta$ , has a light mass with an equal admixture of  $d_{xz}$  and  $d_{yz}$  characters. The also light SOC split-off subband ( $E_\gamma$ ) has a sizable mixture of the three  $t_{2g}$  characters. All these

TABLE I. Calculated zone-center orbital characters including spin index ( $\uparrow, \downarrow$ ) and masses along  $\Gamma X$  of the bulk (“Bulk” entries) and confined bands (“2DEG” entries) for KTO(001).  $\psi_{lb}$ ,  $\psi_{hb}$ , and  $\psi_{so}$  denote the bulk light state, heavy state, and spin-orbit split-off state respectively.  $\alpha$ ,  $\beta$ , and  $\gamma$  are defined in the text. Time-reversal symmetry generates Kramers partners of the above states, with the same energies and masses.

	Eigenstates near $\Gamma$	Masses along $\Gamma X$
Bulk	$\psi_{lb} \sim 0.71(d_{yz}\uparrow + d_{xy}\downarrow)$	$m_{lb} \sim 0.24m_e$
	$\psi_{hb} \sim 0.41(-d_{yz}\uparrow + d_{xy}\downarrow) - 0.82id_{xz}\uparrow$	$m_{hb} \sim 0.66m_e$
	$\psi_{so} \sim 0.58(-d_{yz}\uparrow + id_{xz}\uparrow + d_{xy}\downarrow)$	$m_{so} \sim 0.35m_e$
2DEG	$\psi_\alpha \sim 0.26(d_{yz}\uparrow - id_{xz}\uparrow) + 0.93d_{xy}\downarrow$	$m_\alpha \sim 0.25m_e$
	$\psi_\beta \sim 0.71(d_{yz}\uparrow + id_{xz}\uparrow)$	$m_\beta \sim 0.5m_e$
	$\psi_\gamma \sim 0.66(-d_{yz}\uparrow + id_{xz}\uparrow) + 0.36d_{xy}\downarrow$	$m_\gamma \sim 0.41m_e$

effects result from the comparable magnitudes of the spin-orbit gap in KTO and the Fermi energy and subband splittings of the 2DEG realized at its surface. Experimentally, the  $E_\gamma$  subbands are not observed, as they lie above the Fermi level, and are not considered further.

Additionally, for KTaO<sub>3</sub>, one must take into account the polar character of its surface layers. Statistically one expects that the cleaved surface consists of patches of (TaO<sub>2</sub>)<sup>1+</sup> and (KO)<sup>1-</sup>. This suggests that oxygen vacancies will form preferentially in the negative KO regions. On the other hand, electrons released by the vacancies can populate the subbands on the positive TaO<sub>2</sub> terraces or form polaronlike  $F$ -center states centered on the Ta closest to a vacancy in a KO region. As we will show, all these possibilities are observed in our data.

Figure 2 presents the measured electronic structure of the 2DEG at the surface of KTaO<sub>3</sub>. Figures 2(a)–2(c) show the energy-momentum intensity maps around  $\Gamma_{002}$ ,  $\Gamma_{012}$ , and  $\Gamma_{112}$ , respectively. Their corresponding energy distribution curves (EDCs) are included in the Supplemental Material.<sup>19</sup> Due to dipole selection rules, the relative intensities of the different subbands change across neighboring  $\Gamma$  points and for different photon energies,<sup>24,25</sup> as also observed in the 2DEG at the surface of STO.<sup>13</sup> Figures 2(d)–2(f) show the second derivative of the intensity maps, useful to enhance weak features in the spectra. All these spectra show the existence of at least four subbands with *three* different effective masses: (i) Two very light bands, which we assign to subbands  $E_\alpha^{n=1}$  and  $E_\alpha^{n=2}$  [Figs. 2(d)–2(f)], with band bottoms at  $-370$  and  $-220$  meV and Fermi momenta of approximately  $0.18$  and  $0.14 \text{ \AA}^{-1}$ , respectively. Using a parabolic-band approximation, their experimental effective mass along  $k_y$  is  $m_y^* \approx 0.28m_e$  ( $m_e$  is the free-electron mass), in very good agreement with the mass expected from calculations, as illustrated by the nearest-neighbor two-layer tight-binding fits shown by the dashed red and blue lines in Figs. 2(d)–2(f). (ii) One intermediate-mass band, which we assign to  $E_\beta^{n=1}$ , dispersing down to  $-80$  meV with Fermi momentum  $0.12 \text{ \AA}^{-1}$ , and with experimental mass  $m_y^* \approx 0.7m_e$  (and not  $2m_e$ – $3m_e$ , as incorrectly quoted in Ref. 18), also in good agreement with the calculations

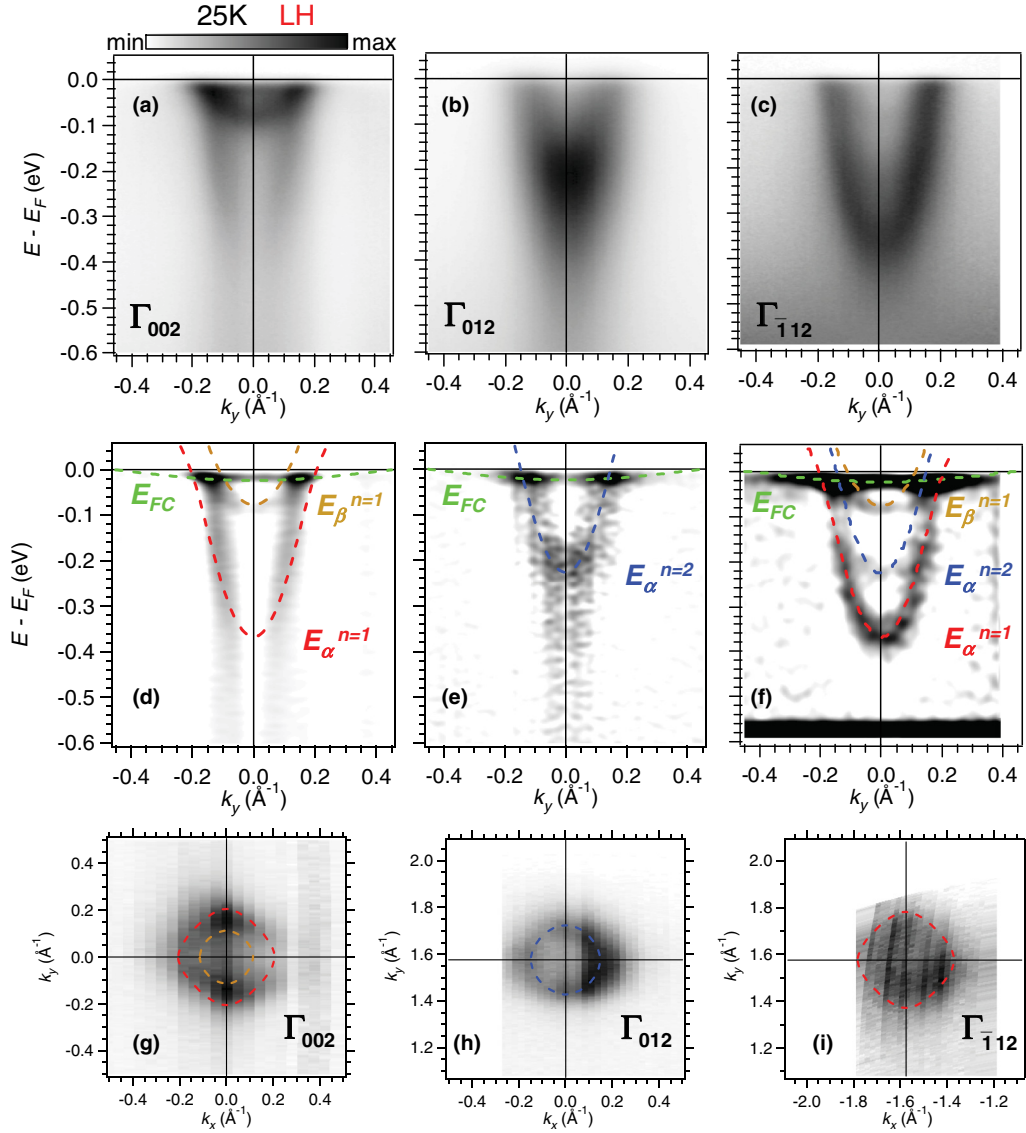


FIG. 2. (Color online) (a)–(c) Energy-momentum intensity maps of the 2DEG subbands in  $\text{KTaO}_3$  near  $\Gamma_{002}$ ,  $\Gamma_{012}$ , and  $\Gamma_{112}$ , respectively. The data were taken along the (010) direction using linear-horizontal photons at 32 eV (a) and 41 eV (b), (c). (d)–(f) Second derivatives (negative values) of the maps in (a)–(c), with tight-binding two-layer fits to the four observed subbands overlaid on the data. (g)–(i) Fermi surface maps around  $\Gamma_{002}$ ,  $\Gamma_{012}$ , and  $\Gamma_{112}$ , respectively, corresponding to the subbands observed in (a)–(c). The Fermi surfaces resulting from the fits in (d)–(f) are also shown.

[dashed orange fit in Figs. 2(d)–2(f)]. Note that this mass is significantly lower, by almost an order of magnitude, than the mass expected from the bulk heavy band, confirming the dramatic combined effects of SOC and confinement discussed in Fig. 1. (iii) One very heavy band, visible in the raw spectra of Fig. 2(a) (or in the corresponding EDCs in the Supplemental Material<sup>19</sup>), and also apparent in the second-derivative spectra [Figs. 2(d)–2(f)]. This band, shown by the dashed green parabola in Figs. 2(d)–2(f), disperses down to only  $-25$  meV, with Fermi momentum  $\sim 0.3$ – $0.45$   $\text{\AA}^{-1}$  yielding an effective mass  $m_y^* \approx 15m_e$ – $30m_e$ . Such a heavy band does not enter the scheme discussed in Fig. 1. We found that its intensity is enhanced at  $h\nu = 32$  eV [Fig. 2(a)], a range not explored in Ref. 18, and strongly decreases (without change in binding energy) for other photon energies. We will show later that

this band arises from shallow  $F$ -center (FC) states in the KO terminations. We denote it  $E_{FC}$ .

Figures 2(g)–2(i) show the Fermi surfaces given by the subbands of Figs. 2(a)–2(c). They consist of a quasidiamond of semiaxis  $\sim 0.18$   $\text{\AA}^{-1}$  [Fig. 2(g)], arising from  $E_\alpha^{n=1}$ , plus two smaller quasicircles of radii  $\sim 0.14$   $\text{\AA}^{-1}$  and  $\sim 0.12$   $\text{\AA}^{-1}$  [Figs. 2(h) and 2(i)], resulting from  $E_\alpha^{n=2}$  and  $E_\beta^{n=1}$ . Note that, due to the strong SOC and orbital mixing, the Fermi-surface ellipsoids, typical of the 2DEG in STO, are not present in KTO. The Fermi surface derived from the band ( $E_{FC}$ ) has a very low intensity, and is difficult to observe.

From the area enclosed by each Fermi surface ( $A_F$ ), the corresponding 2D carrier density is  $n_{2D} = A_F/(2\pi^2)$ . Summing over  $E_\alpha^{n=1}$ ,  $E_\alpha^{n=2}$ , and  $E_\beta^{n=1}$ , and using the lattice parameter  $a = 3.9876$   $\text{\AA}$ , we find  $(0.2 \pm 0.01)e/a^2$  (or

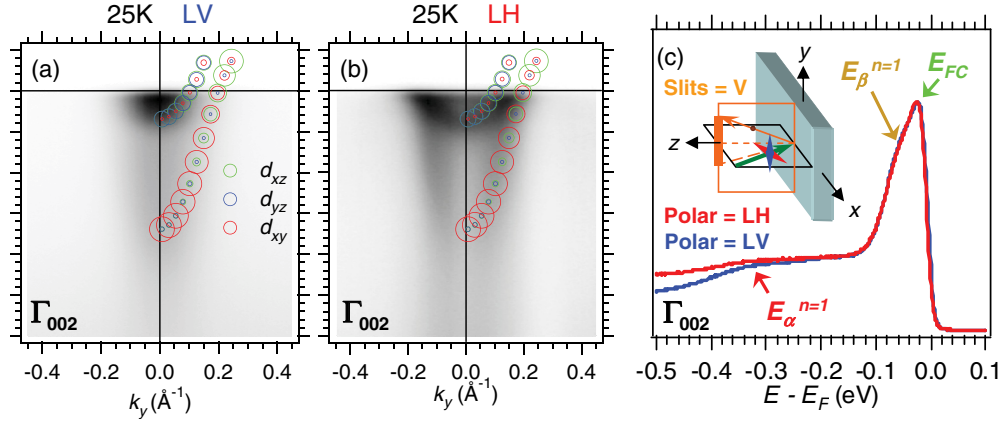


FIG. 3. (Color online) (a),(b) ARPES maps around  $\Gamma_{002}$  along the (010) direction using respectively LV and LH photons at 32 eV. For the  $n = 1$  subbands, the projections on the  $d_{xy}$ ,  $d_{yz}$ , and  $d_{xz}$  characters, extracted from the tight-binding fit of Fig. 1(b), are also shown (open circles). (c) Spectra integrated over  $\Gamma_{002} \pm 0.05 \text{ \AA}^{-1}$  for LV (blue) and LH (red) polarizations. The peaks of different subbands of the 2DEG are indicated by arrows. The inset of (c) shows the geometry for measurements around  $\Gamma_{002}$ .

$\sim 1.26 \times 10^{14} \text{ cm}^{-2}$ ) for the subbands ascribed to the  $\text{TaO}_2$  terminations, similar to reported densities for 2DEGs in STO (Ref. 13) and KTO (Ref. 18). For  $E_{FC}$ , under the assumption that its Fermi surface is circular, we find  $(0.25 \pm 0.1)e/a^2$  ascribed to the KO terminations. Interestingly, such carrier densities are one order of magnitude larger than those one can access with chemical doping, and are similar to those obtained by electrostatic doping to induce superconductivity in KTO.<sup>17</sup> This suggests that cleaving in vacuum might open a route to generate new states of matter, not achievable by bulk doping, in transition-metal oxides.

We ascribe the confinement of the 2DEG to an electric field  $\mathcal{F}$  acting on the charge carriers, following a simple triangular-wedge potential model.<sup>3,13,19,26</sup> As discussed earlier, the subband splittings are given by  $\mathcal{F}$  and the masses along  $z$  of the pure  $t_{2g}$  bands, not by the observed in-plane masses. These parameters can be determined from the data alone: we assume, following the calculations shown in Fig. 1(c), that the orbital character at the bottom of  $E_\alpha^{n=1}$  is essentially  $d_{xy}$ -like (this will be confirmed further), so that its experimental mass of  $0.28m_e$  provides the mass of  $E_\beta^{n=1}$  along  $z$ . Using this mass and the splittings  $E_\beta^{n=1} - E_\alpha^{n=1} = 0.29 \text{ eV}$  and  $E_\alpha^{n=2} - E_\alpha^{n=1} = 0.15 \text{ eV}$ , one obtains  $\mathcal{F} = 280 \text{ MV/m}$  and  $m_z^*(E_\alpha) = 4m_e$ . This mass is in excellent agreement with the one given by the calculations,<sup>19</sup> consistent with the assumption of the bare  $t_{2g}$  heavy mass being the relevant one for the zero-point energies of the subbands. The confining field is  $\sim 3$  times larger than in cleaved STO,<sup>13</sup> possibly due to the dielectric constant of KTO being 2–4 times lower.<sup>27,28</sup> Finally, the width of the 2DEG can be estimated from the spatial extent of the highest occupied subband  $E_\beta^{n=1}$ , yielding  $L \approx 12 \text{ \AA}$ , or about three unit cells.

Our analysis so far does not explain the occurrence of the quasiflat heavy band  $E_{FC}$ . We propose that it arises from electrons released by the oxygen vacancies in the KO terminations. As shown in the Supplemental Material<sup>19</sup> (see also Refs. 17,29–33), these electrons can form atomlike bound states, of energy  $E_a \sim -19 \text{ meV}$  and mean distance  $b \sim 6.6a$  from the position of the missing O, near the Ta that is

directly below the vacancy. Now, from the estimated  $0.25e/a^2$  contributed by the  $F$ -center states, plus the  $0.2e/a^2$  contributed by the 2DEG in the  $\text{TaO}_2$  layers, one obtains a density of about one oxygen vacancy per four surface plaquettes, smaller than  $b$ , hence favoring the formation of a heavy band of bottom energy  $\approx E_a$  out of the above atomlike states (see the Supplemental Material<sup>19</sup>), consistent with the observations. In fact, note that on average the surface would consist of a 50% mix of KO and  $\text{TaO}_2$  units. One could then have a charge transfer mechanism between the KO and  $\text{TaO}_2$  terminations. However, an oxygen vacancy in a KO plaquette, as proposed here, will further help reduce the electrostatic energy of the system.<sup>19</sup> An electrically neutral surface would then correspond to one vacancy every four plaquettes of the mixed surface, in agreement with the experimental estimate. Moreover, the calculations show that the bound state is a 50% linear combination of  $d_{xz}$  and  $d_{yz}$  wave functions. Measurements using different light polarizations, described later, confirm this orbital character.

On the other hand, as in previous reports,<sup>18</sup> we do not observe, within our resolution, any Rashba splitting of the subbands. Our  $\mathbf{k} \cdot \mathbf{p}$  calculations<sup>19</sup> explicitly show that for KTO the linear term in the Rashba splitting exists and is inversely proportional to the gap ( $\Delta$ ) between the valence and conduction bands. Thus, despite the strong SOC and confining field of this system, the very large gap of  $\sim 4\text{--}5 \text{ eV}$  results in a Rashba splitting of a few meV at most. This can be simply understood by noting that the Rashba-induced momentum splitting at the Fermi level ( $k_R$ ) is  $k_R \approx 2e\mathcal{F}/\Delta$ .<sup>22</sup> For  $\mathcal{F} = 280 \text{ MV/m}$  and  $\Delta = 4 \text{ eV}$  this gives  $k_R \sim 0.015 \text{ \AA}^{-1}$ , at the limit of our resolution.

We finally probe the orbital characters of the observed subbands using different light polarizations,<sup>13,24,25</sup> serving as a stringent test to validate our data analysis and interpretation. Figures 3(a) and 3(b) show the energy-momentum intensity maps obtained under linear-vertical (LV) and linear-horizontal (LH) polarizations, defined by the experimental geometry shown in the inset of Fig. 3(c). The detection slits are vertical, defining the plane of detection as the sample's  $yz$  mirror plane. We focus our attention on the data at normal emission

( $k_y = 0$ ), shown in Fig. 3(c), for which the scattering plane of the incident photon and the ejected electron coincides with the sample's  $xz$  mirror plane and has thus a well-defined symmetry. Thus, in order to have a nonvanishing probability for electrons emitted at normal emission, the corresponding dipole transition matrix element between the initial and final states must have a total even symmetry with respect to the  $xz$  plane. Now, the final electron state has to be even with respect to this plane—otherwise the electron wave function would be zero at  $k_y = 0$ . Therefore, for LV polarization, for which the dipole operator is odd with respect to the  $xz$  plane, only the odd  $d_{xy}$ - and  $d_{yz}$ -like initial states can be measured near normal emission. On the other hand, for LH polarization, the dipole operator is even with respect to the  $xz$  plane, and only  $d_{xz}$ -like initial states can be detected at normal emission. From these considerations, the experimental results shown in Figs. 3(b)–3(d) thus confirm that the lowest light band  $E_{\alpha}^{n=1}$ , whose intensity at normal emission is very sensitive to the light polarization, has majority  $d_{xy}$  character near  $\Gamma_{002}$ , while the intermediate-mass band  $E_{\beta}^{n=1}$  and the heavy band  $E_{FC}$ , insensitive to the light polarization, have each *equal weights* of  $d_{xz}$  and  $d_{yz}$  characters.

In conclusion, our results show that the realization of 2DEGs in transition-metal oxides presenting strong couplings between selected electronic degrees of freedom can result in

exotic electronic states *different* from those found in the bulk. In particular, our studies suggest a route for the engineering of the orbital symmetry of the ground state in oxide-based 2DEGs, namely, by designing the confining potential well along the direction for which the desired linear combination of the orbitals in the conduction band has the largest effective mass. Additionally, the observation of a heavy band of  $F$ -center-like states, ascribed to the preferential formation of oxygen vacancies in the KO terminations, suggests that different surface terminations can contribute in different ways to the electronic structure of the 2DEG, and could serve to control its physical properties. All these effects and degrees of freedom offer an exciting playground for the exploration of novel electronic states at oxide surfaces.

This work was supported by the ANR OXITRONICS. A.F.S.S. and M.G. acknowledge support from the Institut Universitaire de France. O.C. thanks Friedrich Reinert for fruitful discussions and the Deutsche Forschungsgemeinschaft for financial support via the Forschergruppe FOR1162. J.G. is supported by ANPCyT (Grant No. PICT-07-837) and CONICET (Grants No. PIP-10-0258 and No. CI-D2052-09). G.H. is supported by the Spanish Government under Projects No. MAT2011-29269-C03-01 and No. NANOSELECT CSD2007-00041.

\*andres.santander@csnsm.in2p3.fr

<sup>†</sup>Present address: CRISMAT, CNRS-ENSICAEN, UMR 6508, 6 boulevard du Maréchal Juin, F-14050 Caen Cedex 4, France.

<sup>1</sup>A. Ohtomo and H. Y. Hwang, *Nature (London)* **427**, 423 (2004).

<sup>2</sup>N. Reyren, S. Thiel, A. D. Caviglia, L. Fitting Kourkoutis, G. Hammerl, C. Richter, C. W. Schneider, T. Kopp, A.-S. Rüetschi, D. Jaccard, M. Gabay, D. A. Muller, J.-M. Triscone, and J. Mannhart, *Science* **317**, 1196 (2006).

<sup>3</sup>K. Ueno, S. Nakamura, H. Shimotani, A. Ohtomo, N. Kimura, T. Nojima, H. Aoki, Y. Iwasa, and M. Kawasaki, *Nat. Mater.* **7**, 855 (2008).

<sup>4</sup>L. Li, C. Richter, J. Mannhart, and R. C. Ashoori, *Nat. Phys.* **7**, 762 (2011).

<sup>5</sup>J. A. Bert, B. Kalisky, C. Bell, M. Kim, Y. Hikita, H. Y. Hwang, and K. A. Moler, *Nat. Phys.* **7**, 767 (2011).

<sup>6</sup>A. Brinkman, M. Huijben, M. van Zalk, J. Huijben, U. Zeitler, J. C. Maan, W. G. van der Wiel, G. Rijnders, D. H. A. Blank, and H. Hilgenkamp, *Nat. Mater.* **6**, 493 (2007).

<sup>7</sup>A. D. Caviglia, M. Gabay, S. Gariglio, N. Reyren, C. Cancellieri, and J.-M. Triscone, *Phys. Rev. Lett.* **104**, 126803 (2010).

<sup>8</sup>M. Ben Shalom, M. Sachs, D. Rakhmilevitch, A. Palevski, and Y. Dagan, *Phys. Rev. Lett.* **104**, 126802 (2010).

<sup>9</sup>S. Okamoto and A. J. Millis, *Nature (London)* **428**, 630 (2004).

<sup>10</sup>A. Kalabukhov, R. Gunnarsson, J. Börjesson, E. Olsson, T. Claeson, and D. Winkler, *Phys. Rev. B* **75**, 121404 (2007).

<sup>11</sup>G. Herranz, M. Basletić, M. Bibes, C. Carrétéro, E. Tafra, E. Jacquet, K. Bouzehouane, C. Deranlot, A. Hamzić, J.-M. Broto, A. Barthélémy, and A. Fert, *Phys. Rev. Lett.* **98**, 216803 (2007).

<sup>12</sup>W. Siemons, G. Koster, H. Yamamoto, W. A. Harrison, G. Lucovsky, T. H. Geballe, D. H. A. Blank, and M. R. Beasley, *Phys. Rev. Lett.* **98**, 196802 (2007).

<sup>13</sup>A. F. Santander-Syro, O. Copie, T. Kondo, F. Fortuna, S. Pailhès, R. Weht, X. G. Qiu, F. Bertran, A. Nicolaou, A. Taleb-Ibrahimi, P. LeFèvre, G. Herranz, M. Bibes, N. Reyren, Y. Apertet, P. Lecoeur, A. Barthélémy, and M. J. Rozenberg, *Nature (London)* **469**, 189 (2011).

<sup>14</sup>W. Meevasana, P. D. C. King, R. H. He, S.-K. Mo, M. Hashimoto, A. Tamai, P. Songsirittigul, F. Baumberger, and Z.-X. Shen, *Nat. Mater.* **10**, 114 (2011).

<sup>15</sup>H. Uwe, K. Oka, H. Unoki, and T. Sakudo, *J. Phys. Soc. Japan* **49** Suppl. A, 577 (1980).

<sup>16</sup>H. Nakamura and T. Kimura, *Phys. Rev. B* **80**, 121308(R) (2009).

<sup>17</sup>K. Ueno, S. Nakamura, H. Shimotani, H. T. Yuan, N. Kimura, T. Nojima, H. Aoki, Y. Iwasa, and M. Kawasaki, *Nat. Nanotechnol.* **6**, 408 (2011).

<sup>18</sup>P. D. C. King, R. H. He, T. Eknapakul, P. Buaphet, S.-K. Mo, Y. Kaneko, S. Harashima, Y. Hikita, M. S. Bahramy, C. Bell, Z. Hussain, Y. Tokura, Z.-X. Shen, H. Y. Hwang, F. Baumberger, and W. Meevasana, *Phys. Rev. Lett.* **108**, 117602 (2012).

<sup>19</sup>See Supplemental Material at <http://link.aps.org/supplemental/10.1103/PhysRevB.86.121107> for more detail.

<sup>20</sup>L. F. Mattheiss, *Phys. Rev. B* **6**, 4718 (1972).

<sup>21</sup>W. A. Harrison, *Electronic Structure and the Properties of Solids: The Physics of the Chemical Bond* (Dover Publications, New York, 1989).

<sup>22</sup>R. Winkler, *Spin-Orbit Coupling Effects in Two-Dimensional Electron and Hole Systems* (Springer-Verlag, Berlin, 2003).

<sup>23</sup>M. S. Dresselhaus, G. Dresselhaus, and A. Jorio, *Group Theory: Application to the Physics of Condensed Matter* (Springer-Verlag, Berlin, 2008).

- <sup>24</sup>S. Hüfner, *Photoelectron Spectroscopy: Principles and Applications*, 3rd ed. (Springer-Verlag, Berlin, 2003).
- <sup>25</sup>A. Damascelli, Z. Hussain, and Z.-X. Shen, *Rev. Mod. Phys.* **75**, 473 (2003).
- <sup>26</sup>T. Ando, A. B. Fowler, and F. Stern, *Rev. Mod. Phys.* **54**, 437 (1982).
- <sup>27</sup>C. Ang and Z. Yu, *Phys. Rev. B* **69**, 174109 (2004).
- <sup>28</sup>R. C. Neville, B. Hoeneisen, and C. A. Mead, *J. Appl. Phys.* **43**, 2124 (1972).
- <sup>29</sup>E. A. Kotomin, Y. F. Zhukovskii, S. Piskunov, and D. E. Ellis, *J. Phys.: Conf. Ser.* **117**, 012019 (2008), and references therein.
- <sup>30</sup>V. V. Laguta, M. I. Zaritskii, M. D. Glinchuk, I. P. Bykov, J. Rosa, and L. Jastrabík, *Phys. Rev. B* **58**, 156 (1998).
- <sup>31</sup>T. Muto, *Prog. Theor. Phys.* **4**, 181 (1949).
- <sup>32</sup>T. Muto, *Prog. Theor. Phys.* **4**, 243 (1949).
- <sup>33</sup>J. Carrasco, F. Illas, N. Lopez, E. A. Kotomin, Yu. F. Zhukovskii, R. A. Evarestov, Yu. A. Mastrikov, S. Piskunov, and J. Maier, *Phys. Rev. B* **73**, 064106 (2006).